DC Microgrids for Ancillary Services Provision, Chapter 15,

Felipe Perez, Gilney Damm, Paulo Ribeiro

Chapter 15

DC Microgrids for Ancillary Services Provision

Filipe Perez[1,3], Gilney Damm[2], Paulo Ribeiro[3]

[1]L2S Laboratory, CentraleSupélec, Paris-Saclay University, France
[2]LISIS Laboratory, University Gustave Eiffel, France
[3]Institute of Electrical Systems and Energy, Federal University of Itajubá, Brazil

Abstract

This chapter is dedicated to DC Microgrid's application to provide ancillary services to weak AC grids. In particular, control algorithms are designed to provide inertial, frequency and voltage support for weak grids, such as AC Microgrids composed mainly by sources interfaced by power converters, with a small portion of diesel generators. A number of synthetic inertia approaches are introduced to improve the stability properties of an AC grid face to strong variations on loads and productions, brought by electric vehicles and possibly other renewable energy sources. The power electronic issues related to control interactions and poor inertial response are described, where suitable solution is addressed. The power converter is driven as a Virtual Synchronous Machine (VSM), where the control strategy follows classical swing equation, such that the converter emulates a synchronous generator, including inertial support. This strategy can be exploited in low inertia systems with high penetration of renewables. An application example illustrates the performance of the Microgrid in the context of virtual inertia control.

Keywords: DC Microgrids, virtual inertia, power system stability, low inertia systems, inertial support, frequency regulation, energy storage systems.

15.1 Introduction

Direct Current (DC) Microgrids are attracting interest thanks to their ability to easily integrate modern loads, renewable sources, Energy Storage Systems (ESS) and Distributed Energy Resources (DER) in general [Ashabani and r. I. Mohamed, 2014, Boicea, 2014]. They also acknowledge the fact that most renewable energy sources and storage systems use DC energy (as Photovoltaic Panels (PV), wind power, batteries and even electric vehicles for example), and allow the reduction of the number of power converters in the grid with simpler topology. By doing this, they increase energy efficiency, and allow faster control of the grid [Tucci et al., 2016, Dragičević et al., 2015, Meng et al., 2017].

DC Microgrids are generally fully composed of DC/DC or AC/DC converters to adapt to the system's voltage level. Commonly, a DC bus operates as the main interconnection link, where power flow control is performed to balance the energy of the system. The devices of the Microgrid are integrated in the DC link to share power, where distributed generators inject the produced power, the

load demand is supplied and the storage elements can absorb the power mismatch. The main target here is to control the DC bus voltage to ensure proper operation of the system, since fluctuations, ripples and deviation in the voltage amplitude may cause a collapse, harming the overall operation of the system. Also, DC/DC converters are used to interconnect buses with different voltage levels, so the devices are inserted according to their voltage level. Therefore, sensitive loads can be properly supplied through a specific bus with multiple DC links configuration [Kumar et al., 2017, Olivares et al., 2014].

On the other hand, the connection of a large number of power converters may lead to stability problems, since the converters can act as a Constant Power Load (CPL), which introduces negative impedance into the system. The effect of the negative impedance reduces significantly the stability margins and the operating region of the entire system. Therefore, standard control techniques, as droop controllers and linear Proportional Integral (PI) controllers, are very limited to attain stability in this case, and different solutions must be achieved to improve the operation of this type of system. The nonlinear control can be introduced as a powerful tool to develop improved controllers, that are robust enough to keep safe operation in a wide operating region. Nonlinear control technique can easily suppress the negative impedance term and insert a stabilizing dynamic through feedback process, when the variables of the system are known [Bidram and Davoudi, 2012, Yang et al., 2016].

In this context, [Bevrani et al., 2017, Sahoo et al., 2017] present a survey on the most relevant features of DC Microgrids, and it is summarized as follows:

1. The reduced number of converters between sources and loads improve efficiency and decrease losses.

2. A number of system variables are eliminated, such as frequency, reactive power, power factor and synchronization.

3. The system is more robust against voltage sags and blackouts, since they have fault ride trough capability from voltage control of the power converter and the energy stored in the DC bus capacitor.

4. DC distribution is not the standard shape and need to be built in parallel to the conventional AC distribution system.

5. The system protection is harmed, since zero cross detection is non-existent.

6. The power electronic loads and DC motors are easily integrated in DC systems, but there are a number of loads that must be adapted for DC power supply.

7. The absence of transformers reduces losses and inrush currents.

8. Voltage stability is directly affected by power flow control.

In the following, some examples of Microgrid studies are mentioned to highlight the possible solutions and improvements in Microgrid topic.

A complete nonlinear model of a DC distribution system driven by PI cascaded droop-based controllers including a damping factor is developed in [Makrygiorgou and Alexandridis, 2017], where a nonlinear stability analysis is conducted using Lyapunov techniques. Also, small signal stability studies are introduced as in [Magne et al., 2012], where different DC loads and a supercapacitor compose the DC network of aircrafts. Then, a large-signal-stabilizing study is proposed to ensure global stability by generating proper stabilizing power references for the whole system. In [Tahim et al., 2015], a simplified model of a small DC Microgrid under droop control is addressed to reduce the complexity of the nonlinear stability analysis, which is based on bifurcation theory, and a relation among grid parameters is provided. Several strategies for stability analysis and stabilization techniques for DC Microgrids are presented in [Meng et al., 2017] and in [Dragičević et al., 2016].

In [Iovine et al., 2017], a nonlinear distributed local control is proposed to interconnect a number of elements in a DC Microgrid. The Microgrid is composed of different time-scale's storage elements, like batteries and supercapacitors that are used to improve the system operation. A stability analysis of the proposed control strategy is conducted considering the system as a whole and its physical limitations. The proposed scheme can easily be scalable to a much larger number of elements and a comparison with standard linear controllers is also carried out. In this way, the control performance

of the system is presented towards interconnected disturbances from loads and PV variations. The robustness of the proposed control is highlighted when compared with linear control. Subsequently, a power management controller to ensure power balance and grid stability of the DC Microgrid is designed in [Iovine et al., 2019]. The secondary control scheme, based on Model Predictive Control (MPC), is developed to optimize the operation of the DC Microgrid in long term, considering weather forecasts and load demand profile. In this case, the power balance and the DC bus voltage regulation are considered as constraints.

Therefore, in [Iovine et al., 2016], the connection with the main AC grid is carried out considering the stability of the Microgrid DC bus, still applying nonlinear control techniques. Afterwards, in [Perez et al., 2018], a more favorable power converter configuration is proposed to improve the electrical scheme of the DC Microgrid. A dynamical feedback controller is designed to reduce the complexity of the stability analysis and simplify previous controller design keeping the stability properties. And finally, a nonlinear control scheme to integrate regenerative braking from a train line is proposed in [Perez et al., 2019b]. In this case, the DC bus stability is also taken into account, where the power surges from braking periods are considered as disturbances. The proposed controller must be able to properly operate regarding various disturbances in the network.

Ancillary services using DC Microgrid is carried out in [Iovine et al., 2018, Perez et al., 2019a], where the available power on the DC side of the Microgrid is used to supply the AC side of the grid appropriately, ensuring voltage limits within grid requirements. Therefore, the power quality of the main grid is improved.

Relating the different applications of power electronics in power systems, High Voltage Direct Current (HVDC) transmission, Multi-Terminal Direct Current (MTDC) and Modular Multilevel Converter (MMC) [Jiménez Carrizosa et al., 2018, Gonzalez-Torres et al., 2020, Chen et al., 2014] results can be adapted for DC Microgrids application, because of the following reasons: they have similar power converter configuration, differentiated only by their size and power value; the electrical model and dynamics of the system are similar; the perturbations' properties can be easily compared to each other; the control schemes are compatible, besides the gain tuning.

The main challenge in the operation of Microgrids is to maintain a safe operation of the system, balancing generation and demand, where the optimal management of the system can be done through heuristic algorithms or intelligent control. The Microgrid operation address different energy scenarios, where generation excess/deficit is minimized through optimization methods composed of cost functions. However, the open-loop feature of optimization systems does not allow to compensate uncertainties and disturbances. Therefore, MPC closed-loop feature allows corrective actions using measurements to update the optimization problem, which ensures the optimal operation of the system [Bordons et al., 2020, Parisio et al., 2014].

The hierarchical control structure of Microgrids performs the separation of the variables according to time-scales, therefore variables with close time responses are controlled in the same control level. Hierarchical control are typically composed of three different levels: primary, secondary and tertiary level. Primary control deals with the stability of currents and voltages at the transient level, on a time-scale from milliseconds to seconds. The secondary control performs the control of power and energy of the system through optimization techniques in minutes to hours. The tertiary control deals with strategic dispatches, according to an energy market or human factors, in the range of hours or days [Vasquez et al., 2010, Arnold et al., 2009]. A general scheme of a Microgrid is presented in Figure 15.1, where the Microgrid central control contains the hierarchical structure to optimal operation of the entire system.

15.1.1 Droop control strategy

Droop control strategy traditionally applied in AC Microgrids is also widely applied in DC Microgrids for power sharing purposes. This simple strategy is based on the linearized behavior of the system power flow around a operation point. The output power/current can be used as the droop feedback. In the Power-based droop, the DC bus voltage reference is given by the power variation in the grid according to the droop coefficient [Tayab et al., 2017, Tahim et al., 2015, De Brabandere et al., 2007].

$$V_{DC,ref} = V^*_{DC} - m_p P_{out} \tag{15.1}$$

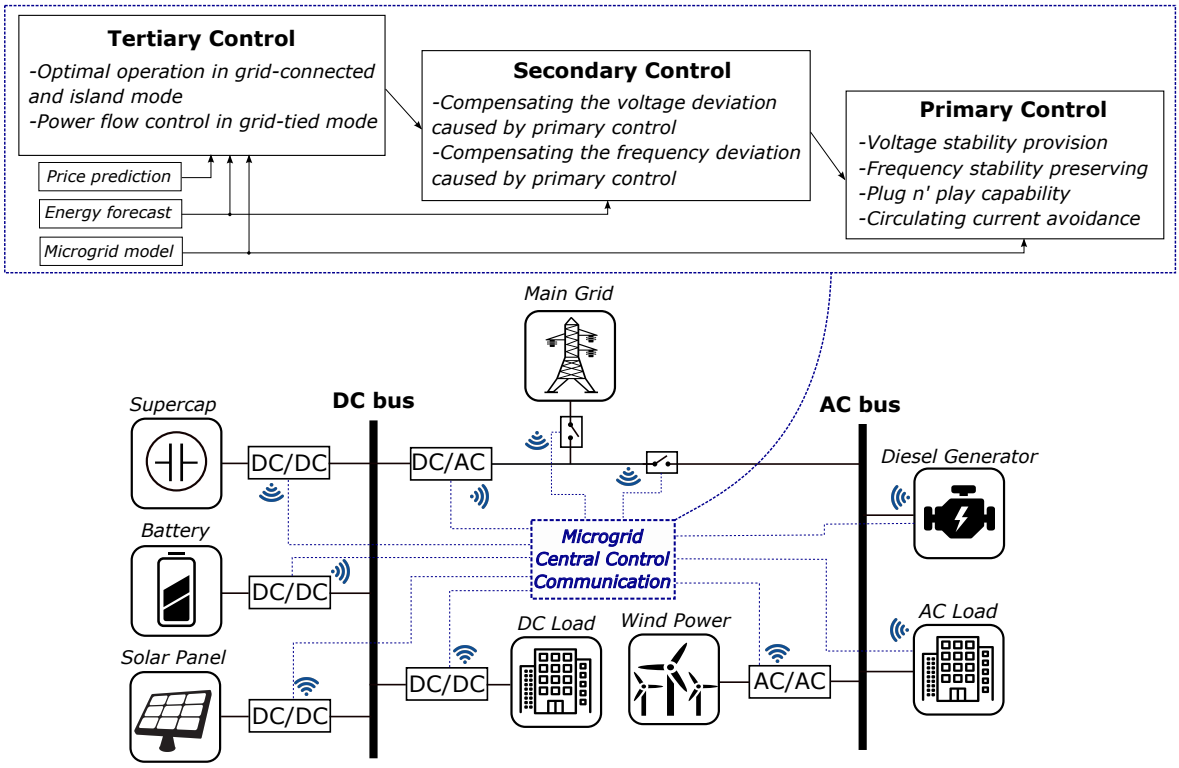

Figure 15.1: A Microgrid composed of central control with hierarchical structure.

where $V_{DC,ref}$ is the voltage reference value for the given operation condition, V^*_{DC} is the rated DC voltage value. m_p is the droop coefficient and P_{out} is the power output.

In the Current-based droop, the DC bus voltage is the control output, given by the droop coefficient and the current in the converter.

$$V_{DC,ref} = V^*_{DC} - m_i I_{out} \tag{15.2}$$

here, $V_{DC,ref}$ is given by the droop relation according to the current output I_{out}. m_i is the droop coefficient, which can be interpreted as a virtual internal resistance. A general control scheme of the conventional droop control is introduced in Figure 15.2 according with [Dragičević et al., 2015].

The droop strategy is associated as an adaptive voltage positioning and the droop coefficients have a direct effect over system stability and power sharing accuracy. Higher droop coefficients may bring better sharing accuracy and damped response, but a commitment must be made not to cause major voltage deviations. Besides that, the droop coefficient can change the power sharing of the generation units.

An extension of conventional droop control is to introduce adaptive feature for droop control, where the droop coefficients become time varying ($m_p(t)$ and $m_i(t)$), and can change according to a specific strategy. The adaptive calculation of droop control can consider the State-of-Charge (SOC) of the ESS or other strong perturbations related to power injection and load demand. With the dynamic adjustment of the coefficients, the operation of the system and power sharing is improved. This approach also reduces the effects of the line impedance and also reduce line losses, but the control parameterization is too complex [Tayab et al., 2017].

15.1.2 Power System Problems

Historically, power systems were based on synchronous machines rotating in synchronism, sharing power to supply the load, and providing natural inertia (frequency response) following disturbances or simply changes on operating conditions. This classical scheme is less and less true, because of the large penetration of power electronic devices like power converters and modern loads.

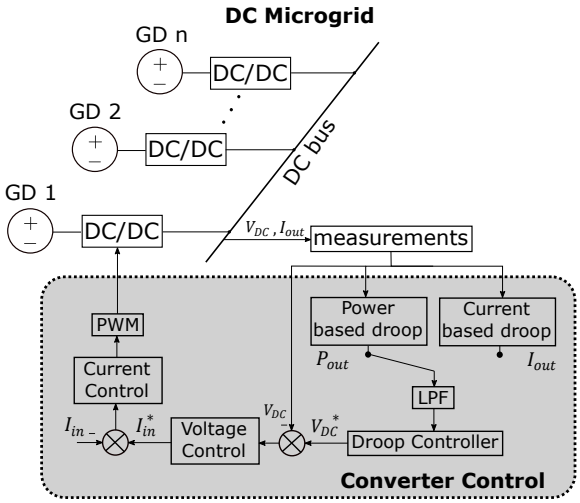

Figure 15.2: Conventional droop control scheme for multiple generations units in a DC Microgrid.

Power converters are inherent to the interconnection of renewable energy sources and storage units as mentioned before, but also by the HVDC lines that are being built to reinforce current transmission systems. For this reason, inertia is reducing fast, and in some situations, there are grids mostly composed of power converters where the frequency reference is completely lost [Tielens and Van Hertem, 2016, Winter et al., 2014, Milano et al., 2018]. This situation is a change of paradigm from the classic electric grid, and power systems practitioners are struggling to keep the grid running. A recent example of such situation is the 9 august 2019 black-out in the United Kingdon [National Grid ESO, 2019], where arguably the main cause was the reduction of inertia, and its effect in several power converters interconnecting distributed generation.

Distributed generation are mostly formed by renewable energy sources, which have power electronics interface. And so, the power converters do not have an inertial response due to the absence of a rotating mass, as conventional synchronous generators do. Power converters are unable to naturally respond to load change. Consequently, the frequency response worsens, causing oscillations and operating margins problems. Thus, the integration of renewables has a direct relationship with the reduction of inertia in power systems.

The inherent features for systems mainly composed of power converters are:

1. Fast response;
2. Lack of inertia;
3. Harmonic issues;
4. Interaction between controls;
5. Weak overload capacity.

The converter dominated grid is emerging from a traditional generator dominated grid, therefore the lack of inertia is becoming a main issue of concern. The grid modernization through power electronics advancements is a trend research topic in power systems related to Smart Grids. In this way, energy storage is required to balance generation and consumption in this kind of system, specially for strong variations on load or generation, when compared to the case of rotating mass reserve (inertia) and damping winding in traditional synchronous machines that buffer the strong oscillations maintaining the system's stability.

15.2 Ancillary Services in Brazil

The main responsibility of a Transmission System Operator (TSO) is to provide electric power from generators to the consumers through transmission lines meeting the standardized network requirements (*grid codes* - obligations of control areas and transmitting utilities) to maintain the proper

and reliable operation of the system interconnection. In this context, the specific services and functions provided to maintain and support the power supply in the grid are called ancillary services. Ancillary services support the grid to maintain continuous and reliable operation of the system, properly supplying the loads while keeping stability and security. Traditionally, ancillary services are provided by generators controlled by the TSO, however the integration of power electronic based equipment in the network expanded the possibility of ancillary services provision. Therefore, power electronic devices and generators non-controlled by the TSO are now able to participate on the support to the grid in several operation modes, which has created a new opportunity in the energy market [Joos et al., 2000, Wu et al., 2004, Rebours et al., 2007].

The ancillary services provision in Brazil is still very limited because of regulation aspects and restricted to the generation units controlled by the TSO (composed of hydroelectric and thermoelectric plants). There are some generation units able to operate as synchronous compensators, which provide reactive power compensation through a formal contract with the national TSO. These are centralized thermoelectric plants used as operational power reserves. Therefore, power plants non-controlled by the TSO cannot perform ancillary services, which greatly restrict these services in Brazil [ANEEL, 2018, ANEEL, 2019a, ANEEL, 2019b].

According to [ANEEL, 2019a], the ancillary services' provision in Brazil includes the following supports: a) Primary frequency control, performed by all generating units integrating the national electrical grid; b) Secondary frequency control, where only the plants that are part of the Automatic Generation Control, requested by the TSO participate; c) Reactive power support, performed by generation units integrating the network and by plants that operate as synchronous compensators, under prior authorization from the National Electrical Energy Agency (ANEEL); d) Black-start, performed by all generation units integrating the network and by plants in compliance with ANEEL, and on demand from the TSO; e) Complementary power reserve dispatch, performed by centrally dispatched thermoelectric plants.

In this context, the report in [ANEEL, 2019b] proposes a normative review for ancillary services provision based on the reduction of the regularization of the reservoirs of hydroelectric power plants and the high penetration of intermittent renewable sources. It is also proposed to encourage the expansion of existing services (mentioned above) and the insertion of new services such as:

1. Development of new services for reactive power compensation using photovoltaic plants, reactive power support for wind power plants and even in the distribution system;

2. Inertia as an ancillary service through power electronics equipment, aiming at reducing the connection of thermal plants;

3. Load modulation by distribution agents, performed through the dispatching of power plants not operated by the national operator, but by the local distributor;

4. Paying for ancillary service provision: payment through ancillary services' charges by bilateral negotiation between consumer and the provider, raising the need for the development of an ancillary services market.

Thus, in the Brazilian scenario, there are still many barriers to the diversification of ancillary services provision, being restricted to large generation units controlled by the TSO. Also, technological adaptation costs and equipment deterioration costs combined with massive insertion of power electronics' devices and communication equipment make the valuation of ancillary service provision quite complex.

15.3 Power Converter Issues

As explained above, recent grid evolution has brought the integration of renewable energy sources, ESS and loads based on power electronics. But these power converters have different behavior than synchronous machines. Synchronous machines have an inherent energy storage from their rotational mass[1], being able to naturally respond to a load disturbance contributing to system stability, while

[1]Synchronous generators store kinetic energy proportional to moment of inertia J and the square of their angular speed, with time response of few seconds.

power converters are directly affected by their controllers with fast response and very low natural energy stored[2]. Therefore, power converters do not have the natural ability to contribute to frequency stability in the active power sense [Poolla et al., 2019, Pattabiraman et al., 2018].

In Microgrids context, power converters use the measured voltage of the network to estimate the phase angle of the grid, being able to synchronize with the main grid to generate the voltage output, i.e., grid-following converters. The main issue related to power converters in Microgrids is the difficulty to implement isolated operation called as grid-forming converters. Grid-forming converters are a great concern in academia and industry, where numerous studies have been carried out to develop useful strategies to proper operate electrical grids only composed of power electronics technologies. In this context, droop control has been widely applied, since it allows power share among power converters with a distributed control approach.

A crucial issue in power electronics technology is the lack of inertia and interactions between control as stated by the United Kingdom Transmission System in [Grid, 2014]. In fact, the high penetration of power electronics based technologies decrease the inertia of the system, bringing frequency stability problems and reduction of transient stability margins.

The AC/DC power converters like Voltage Source Converters (VSC) are mostly controlled by Pulse-Width Modulation (PWM) and traditional control schemes in grid-following operation make these converters behave as current sources[3]. The Phased-Locked Loop (PLL) is used to synchronize the converter with the grid by estimating the phase angle of the network, where the calculation of the voltage reference depends on the grid impedance. Therefore, the control performance is affected by grid impedance, which makes these control schemes sensitive to grid condition. So, it is necessary to design a good interaction between the PLL, voltage and current control loops, PWM switching frequency and the output filter. The match of controllers' bandwidth can be a very complex task. Usually, current control loop bandwidth is tuned twenty times smaller than the PWM frequency and filter frequency is designed accordingly [Jessen et al., 2015, Breithaupt et al., 2016].

Other important issues can be related to power electronics in power systems, where countries in Europe are dealing as priorities [Rodrigues Lima, 2017]:

1. Decrease of inertia, related to frequency stability;
2. Wrong participation of power converters devices in frequency regulation (control errors);
3. Reduction of transient stability margins due to decreased short-circuit capacity of power converters
4. Resonance and oscillations caused by power electronics;
5. Power electronics controller interaction among the devices (active and passive) in the grid.

In this scenario, new ancillary services and grid support are needed to fulfill the stability requirements for power system operation and reliability. A suitable solution is to develop new control strategies for power converters changing the original feature of power converters to provide ancillary services to the network and reduce the power electronics impacts [Joos et al., 2000].

Traditional power systems composed of synchronous generators have a well established time-scale separation considering the dynamics of the system. Usually, the time constant for frequency and voltage regulation are related to slow dynamics of turbines (about $10s$) and governors (about $1s$), compared with faster dynamics of the exciter (about $50ms$), which can deal with the network line dynamics (time constants about $1-30ms$). Besides that, the time constant of the swing equation and flux linkages will be given by the flux and swing dynamics. So, in conventional systems, the controllers are typically designed considering its operational margins and can assure the stability of the whole system. However, in low inertia systems, the fast dynamics of power converter-based generation bring interactions among different controllers, affecting the time-scale separation and increasing complexity [Markovic et al., 2019].

The time-scale separation of power systems including power converter-based generation and the dynamics feature of low inertia are introduced in Figure 15.3, adapted from [Markovic et al., 2019].

[2]The capacitors of power converters can store electrostatic energy in order of units to hundreds of milliseconds.

[3]Usually, VSC have outer voltage control loop and an inner control loop, which is the current control loop

It is presented the physical and control dynamics, considering three different time-scales: signal processing, voltage dynamics and frequency dynamics. The voltage and frequency dynamics are related to the controllers designed for these purposes. The signal processing is associated to the fastest interactions ($< 1ms$), which may include PWM signals and harmonics from converters, and fiber optics network communication. Then, the voltage dynamics are associated with larger range time-scale interactions ($> 1ms$ to $< 100ms$), which includes the network line dynamics, Automatic Voltage Regulator (AVR), Power System Stabilizer (PSS), linkage flux dynamics of synchronous machines, and the Synchronous Reference Frame (SRF) inner control loops of converters. The frequency dynamics are associated with the slowest interactions ($> 10ms$ to $10s$), including the Active and Reactive Power Control, PLL of power converters, Governors, Turbine and swing dynamics of synchronous machines [Markovic et al., 2019, Kundur et al., 1994, ENTSO-E, 2013].

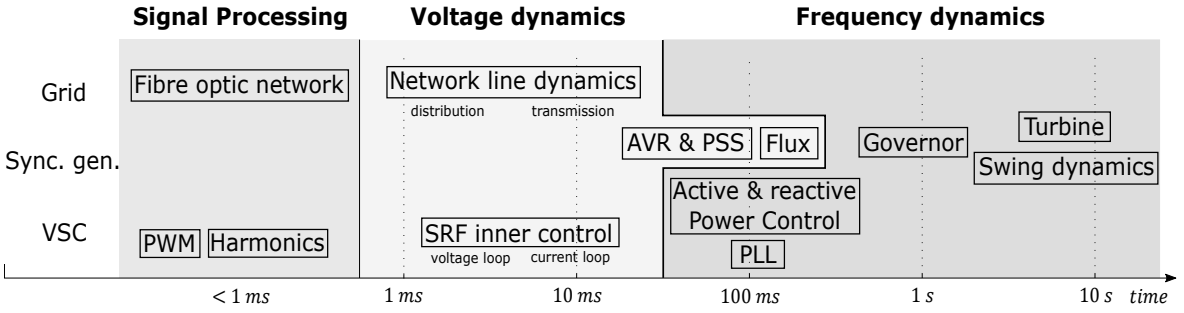

Figure 15.3: Time-scale separation of power system dynamics considering conventional synchronous generators and power converters integration.

In this sense, the controllers and Low-Pass Filter (LPF) of power converters have faster dynamics than synchronous generator controllers, resulting in control interactions and causing stability issues, since they have different time constants as shown in Figure 15.3. So, power converters can potentially impact in the frequency regulation in low inertia systems, affecting frequency dynamics and the associated fast transients. The result is the deterioration of protection schemes that consider the limitation of frequency Nadir[4] and Rate of Change of Frequency (RoCoF) due to incompatible control strategies interacting with the main grid under high penetration of power electronic-based generators. The transmission line dynamics also interact with the dynamics of power converters' controllers, where the fast behavior of these dynamics can amplify the interactions. Therefore, when the X/R impedance ratio is high enough, the time constant of the line is able to suppress the gap between faster dynamics of power converters and slow dynamics of synchronous generators, acting as a buffer, improving the system stability. However, in distribution lines, the lower X/R relation restricts the operation and control of voltage and frequency, hindering system's stability. In this case, virtual impedance application may be a feasible solution for these stability issues.

15.3.1 Inertial response and low inertia issues

Since power converters' based generation is not able to provide natural frequency support (sub-second and primary controls), the reliability of renewable generators and Microgrids can be dramatically reduced. Consequently, the frequency response of the system as a whole can be affected, which is an European concern [Breithaupt et al., 2016].

A reduced inertia may cause higher frequency excursions during and after a contingency and also increase the RoCoF. RoCoF is used to indicate load disconnections (Load Shed) and in protection schemes to detect the disconnection of generation units. Therefore, faster frequency ancillary services, inertial response emulation and increase of grid code requirements for RoCoF were proposed by [Grid, 2016, Eirgrid, 2012].

The active power response for a system with inertia (natural or virtual) depends on its inertial constant (H) and the derivative of frequency as:

$$\Delta P_{p.u.} = -\frac{2H}{f_0}\frac{df}{dt} \tag{15.3}$$

[4]Frequency Nadir is defined as the minimum value of frequency reached during the transient period.

where f is the measured frequency and f_0 is the nominal grid frequency.

The inertial power variation ($\Delta P_{p.u.}$) is proportional to the RoCoF, then its maximum is just after a frequency disturbance and it goes to zero when a new equilibrium point is reached. Let us consider a disturbance like a load increase (or generation loss) in a power system with primary reserve used to hold the frequency drop. The behavior of frequency deviation and the inertial power variation are depicted in Figure 15.4 from [Rodrigues Lima, 2017]. In this case, the frequency Nadir is reduced when the inertial support takes place, which means that inertial power helps to improve frequency variations.

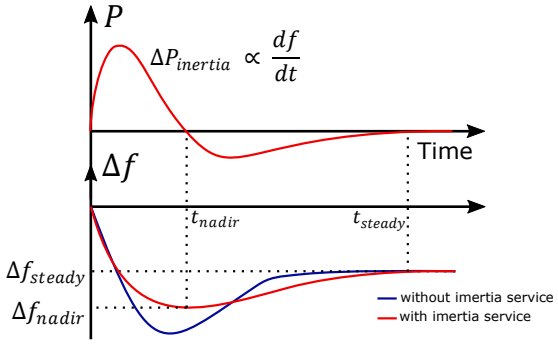

Figure 15.4: Inertial response scheme with a primary control.

This is a natural response of synchronous machines, but power electronics devices may mimic this phenomenon as a virtual inertia approach. The synthetic inertial response after a contingency can be a very good solution to systems presenting lack of inertia due to power electronics interfaced connections, since it results in an equivalent behavior of synchronous machines. The main difficulty in this process is to measure the frequency, when it is not possible to use the angular velocity of a synchronous machine (Power converters based grids). Therefore, the PLL can be used for frequency measurement in this case.

15.3.2 Frequency problems in weak power systems

Frequency stability issues caused by power converters have stronger impacts in weak grids and Microgrids, since they already have small inertia constants. Anyhow, reduction of system's inertia affects frequency deviations even in strong grids, since the arrival of renewables. The Electricity Reliability Council of Texas (ERCOT) has reported a continuous decline in the inertial response of its system and recommends additional inertial response [ERCOT, 2013]. Also, the European Network of Transmission System Operators for Electricity (ENTSO-E) has reported frequency violations growth related to large renewable integration in the grid [ENTSO-E, 2017]. So, frequency problems have a straight relation to renewables penetration and power converters based grids.

Frequency limits are imposed by TSOs, and these limits are well defined in grid codes. For example, the IEEE recommends a tight frequency operating standard of $\pm 0.036\ Hz$ for grid-connected systems, but for off-grid operation in Microgrids and isolated systems, the limits are redefined to fit limitations of this kind of operation. In the North American Reliability Corporation (NERC) the recommendation is to start load shedding when the frequency drops bellow 59.3 Hz to re-balance the system[5]. For variations lower than 57 Hz or higher than 61.8 Hz, the NERC recommendation is to disconnect generators units. To highlight the regulatory differences between grid-connected and isolated modes, Table 15.1 is introduced from [Tamrakar et al., 2017]. Generally speaking, the limits for island mode are relaxed compared with grid-connected mode, allowing variations of $\pm 1.5 Hz$ in frequency, and up to $\pm 9\ Hz$ for critical periods according to ISO 8528-5 standard, which provides a guideline for frequency in off-grid context.

[5]Nominal frequency in this case is 60 Hz.

Table 15.1: Microgrid operation standard for frequency levels.

Grid-connected	**Island mode**
Frequency: main grid task	Freq. primary controller by VSC
Small number of critical deviation	Low inertia with critical deviations
IEEE	**ISO 8528-5**
Recommended range: $\pm 0.036\ Hz$	Nominal range: $\pm 1.5\ Hz$
NERC	Critical range: $\pm 9\ Hz$
Freq. < 59.3 load shedding	Recovery time: $10\ s$
Freq. < 57 or > 61.8 disconnect generator	Maximum RoCoF: $0.6\ Hz/s$
EN50160	
49.5 to 50.5 Hz for 95% of a week	
47 to 52 Hz for 100% of a week	

15.4 Virtual Inertia and Inertial Support

Virtual or synthetic inertia consists in emulate in power electronic devices the energy stored in rotational mass (inertia) of synchronous generators, such that the power converter is able to have natural frequency response. The definition of Synthetic Inertia from [ENTSO-E, 2017] is:

"A facility provided by a Power Park Module or HVDC System to replace the effect of Inertia of a Synchronous Power Generating Module to a prescribed level of performance."

The concept of virtual inertia implementation through power converters has first appeared in [Beck and Hesse, 2007]. The synchronverter concept was then developed [Zhong and Weiss, 2010], subsequently called as Virtual Synchronous Machine (VSM)[6] in [Sakimoto et al., 2011]. These are composed by power converters that mimic or behave like synchronous machines. In this way, it is much easier to integrate such systems to the power network, providing a framework that practitioners are well acquainted with [Van et al., 2010, D'Arco et al., 2015b, Tamrakar et al., 2017]. These VSMs have raised much interest in recent years and have been widely applied to improve frequency stability and to provide inertial support in weak grids and Microgrids [Torres and Lopes, 2013, Shrestha et al., 2017, Zhong, 2016].

Virtual inertia uses a combination of control strategies, Distributed Energy Resources (DER), as renewables and storage systems, and power converters to emulate the inertia of conventional synchronous machines. The control algorithm for virtual inertia approach can be implemented in a power converter, where the mathematical equations describing the inertial response are used to synthesise the control signal sent to the converter. Therefore, power converters become capital devices able to emulate inertia based on a control scheme. PV's and ESS with VSC converters (inverters), wind turbines with back-to-back converters and even HVDC links with multilevel converters can apply the virtual inertia approach to contribute with inertial response for the grid. The key element to emulate inertia in this case is the available energy from DER to proper inject power following inertial feature [Poolla et al., 2019, Tamrakar et al., 2017, Bevrani et al., 2014].

VSM reproduces the dynamic properties of a real synchronous generator in a power electronic unit, in order to achieve the inherent advantages of a synchronous machine for stability improvement. It can be applied in either strong grids on power converters based integration or in Microgrids.

The inertial response of a typical power system is given in less than ten seconds duration, where the synthetic inertia approach provides its contribution to improve system stability. The frequency Nadir can be greatly reduced along with high RoCoF thanks to inertial behavior created by this approach. Virtual inertia features can also improve the governor response, highlighting its contribution to primary control in general. Therefore, virtual inertia must operate in a short time range in autonomous way like inertial response from synchronous generators. The advantage here is that the inertial time response (H) can be adjusted as needed[7], and even can become a state variable to behave, such that, frequency stability is improved.

[6] Note that VSM is said as the VSC operating as a synchronous machine.
[7] The comparison can also be done with moment of inertia J.

15.4.1 Virtual inertia topologies

The basic concepts of virtual inertia in the literature are quite similar, even because as shown above, its definition is related to its effect and not to the means to obtain it. Hence, there are various topologies distinguished by their model and implementation strategy. A topology may mimic the exact behavior of a synchronous machine, by applying the mathematical model of such machine, while other approaches applies directly the swing equation of synchronous machines to simplify the implementation on power converters, and yet others incorporate a responsive DER to respond to frequency changes. Next, the main topologies described in literature are discussed.

Synchronverter

Synchronverters developed in [Zhong and Weiss, 2010] are based on the dynamical equations of synchronous machines from the network point-of-view. Such control strategy allows a traditional operation of the power system without major changes in the operational infrastructure. The electrical torque (T_e), terminal voltage (e) and reactive power (Q) result from the equations written in the converter such that, a synchronous generator behavior is captured. A frequency droop strategy is applied to regulate the output power from the converter. The equations to model the synchronverter are:

$$T_e = M_f i_f i_g \sin\theta \tag{15.4}$$

$$e = \dot{\theta} M_f i_f \sin\theta \tag{15.5}$$

$$Q = -\dot{\theta} M_f i_f i_g \cos\theta \tag{15.6}$$

where M_f is the magnitude of the mutual inductance between the field coil and the stator coil, i_f is the field excitation current, θ is the angle between the rotor axis and one of the phases of the stator winding, and i_g is the stator current.

Figure 15.5 presents the block diagram of the proposed control scheme of a synchronverter presented in [Zhong and Weiss, 2010], where i and v are the current and voltage feedback used to solve the equation within the controller. J is the moment of inertia and D_p is the damping factor, which are arbitrary control parameters used to impose desired dynamic behaviour. The design of these parameters is intrinsically related to the stability properties of the system and will dictate the RoCoF, frequency Nadir and power injection limits to keep the grid requirements.

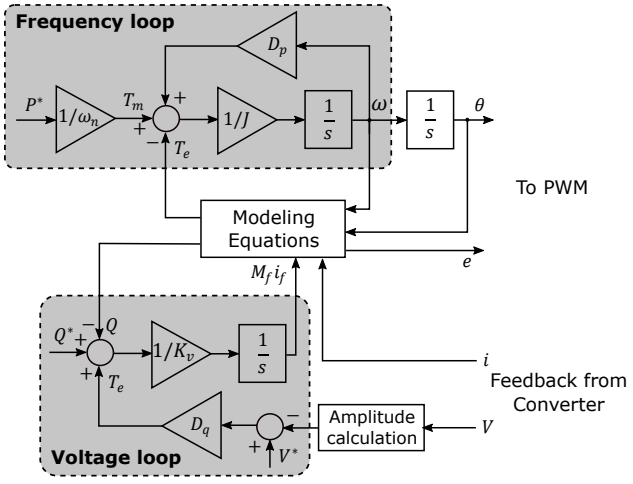

Figure 15.5: Control diagram of a synchronverter.

The frequency and the voltage loops are used to generate the control inputs: mechanical torque T_m, given by the active power reference P^* from the swing equation and excitation variable $M_f i_f$, given by the desired voltage amplitude in the terminal v^* and the reactive power reference Q^* from the droop strategy. The voltage loop have a droop constant D_q, where the measured reactive power is compared to its reference (Q^*). The resulted signal is then integrated with a gain K_v to eliminate

steady-state error, resulting in $M_f i_f$. With $M_f i_f$, it is possible to generate e, which is the first control output for the converter related to the modulation index (voltage amplitude regulation). A virtual angular frequency is generated (ω) from the swing equation loop, hence its integral θ can be calculated to be the reference for PWM, which is the second control output of the converter related to power injection.

In the synchronverter topology, PLL is only used for initial synchronization and frequency measurement purposes, since the frequency loop from swing equation generates a natural ability to attain synchronism with the terminal voltage. A self-synchronized version of this approach is introduced in [Zhong et al., 2013], greatly improving the stability performance, because PLL application may lead to instabilities in weak grids. In the synchronverter topology, the frequency derivative is not necessary for the control implementation, which is a great advantage since frequency derivative computation may bring noise and poor control performance. Another great advantage is the fact that voltage source implementation allows grid-forming operation for isolated systems. Synchronous motors can also be obtained when this topology is applied to the power electronic based loads (rectifiers), helping with inertial response in the load side [Ma et al., 2012]. Concluding, synchronverters is seen as a great solution for power converters based application in power systems to improve system's stability.

ISE topology

The ISE lab topology is based on the swing equation of a synchronous machine, where the power-frequency relation is used to emulate the inertial response of the system [Sakimoto et al., 2011]. In this strategy, the voltage v and current i on the output converter is measured to compute the grid frequency ω_g (which can be done by the PLL) and the active power output P_{out}. The swing equation of this approach is written as follows, where the phase angle θ can be computed to generate the signal for PWM:

$$P_{in} - P_{out} = J\omega_m \frac{d\omega_m}{dt} + D_p(\omega_m - \omega_g) \tag{15.7}$$

where $\theta = \int \omega_m dt$, P_{in} is the active power input given by the prime mover and ω_m is the virtual rotor speed.

A governor model is used in this case to control the grid frequency (ω_g) to its reference ω^*. The prime mover power input reference P_{in} is computed by a first order system with gain K and time constant T_d, where P_0 is the active power reference received from a higher level controller.

$$P_{in}(s) = P_0(s) + \frac{K}{1 + T_d s}[\omega^*(s) - \omega_g(s)] \tag{15.8}$$

The voltage reference (e), can be implemented via $Q - V$ droop control to generate the amplitude reference for the PWM. Similarly, $P - f$ droop control may be applied to generate the power reference P_{in} instead of a prime mover approach. The general scheme of ISE topology is illustrated in Figure 15.6 from [Tamrakar et al., 2017].

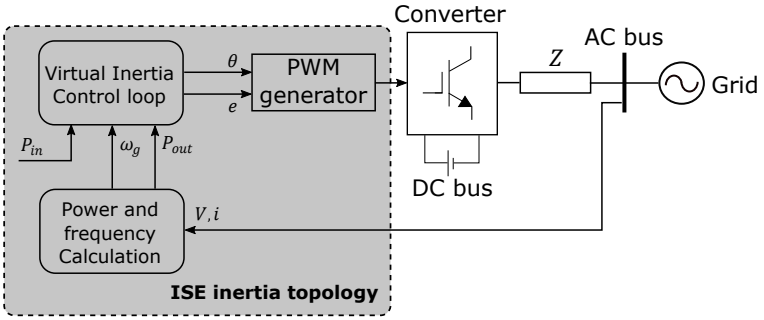

Figure 15.6: General control scheme of ISE lab topology for virtual inertia.

As in the synchronverter approach, frequency derivative is not required in the present case, what improves the control performance, avoids signal pollution and can be applied for grid forming units. Nevertheless, a poor design of swing equation parameters (J and D_p) may result in oscillatory behavior and instability problems.

Virtual synchronous generators

Virtual Synchronous Generators (VSG) is a Frequency-Power response based topology that emulates the inertial response feature of synchronous generators focused on frequency deviation improvement. It is a simple way to insert inertial characteristics in power converter units[8], since it is not necessary to incorporate the detailed equation of synchronous generators. VSG can be easily compared with standard droop controllers, but they can also provide dynamic frequency control, unlike droop controllers that only have steady-state performance. The dynamic frequency control is implemented by frequency derivative measurement, where the system reacts to a power imbalance [Van Wesenbeeck et al., 2009, Torres and Lopes, 2009]. So, VSG provides a power output (P_{vsg}) according to frequency deviation, which equation is written as follows:

$$P_{vsg} = K_D \Delta\omega + K_I \frac{d\Delta\omega}{dt} \tag{15.9}$$

where $\Delta\omega = \omega - \omega^*$ is the frequency deviation and $d\Delta\omega/dt$ is the RoCoF. The gains K_D and K_I represents the damping factor and the inertial constant respectively, based on a synchronous generator model.

The inertial constant (K_I) impact the RoCoF improving the dynamic frequency response, which is a suitable solution for isolated systems where the RoCoF may have high values, harming system stability. Therefore, this approach can be applied to enhance RoCoF values, and the damping constant (K_D) have the same effects of a $P - f$ droop controller. In this topology, a PLL must be used to measure frequency deviation and RoCoF, which can be challenging, since the harmonic distortions and voltage variations may lead to poor control performance, while, in the other topologies, PLL is not really necessary. The VSG scheme is depicted in Figure 15.7 adapted from [Tamrakar et al., 2017].

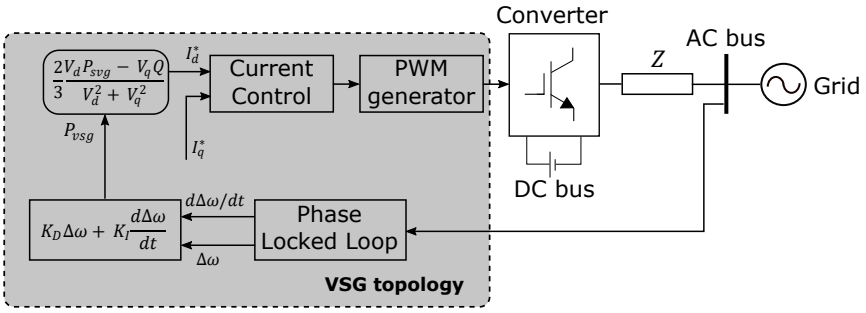

Figure 15.7: General control scheme of VSG topology for virtual inertia.

VSG can be seen as a dispatchable current source, where P_{vsg} is used to calculate the current reference for power converter control loop. Equation (15.10) presents the current reference I_d^* related to active power injection:

$$I_d^* = \frac{2}{3}\frac{V_d P_{vsg} - V_q Q}{V_d^2 + V_q^2} \tag{15.10}$$

where V_d and V_q are the voltages in dq reference frame from Park transformation, Q is the measured reactive power.

The reactive power can also be controlled by calculating current reference I_q^* related to reactive power injection:

$$I_q^* = \frac{2}{3}\frac{V_d Q^* - V_q P}{V_d^2 + V_q^2} \tag{15.11}$$

where Q^* is the reactive power reference, which may be obtained by a droop control strategy, and P is the measured active power in the grid.

VSG topology is used by the European VSYNC group, because of the simplicity and effectiveness features of this approach. When applied as current sources as described in equations (15.10) and

[8]Power converter units can be understand as a generalization for DER integrated via power converters.

(15.11), VSG approach is not able to operate as grid-forming unit. Also, the inertia is not emulated during power input variations, but only in frequency variations. And the main problem of this approach is the complexity to compute and measure frequency deviations and RoCoF, since the derivative operation involves noise pollution and stability issues[9]. Stability problems can also be noticed, when cascaded control loops are used, such as PI controllers with an inner-current loop and an outer-voltage loop for converters. This happens because the gains of these controllers may be complex to tune, which results in inaccurate control performance [Midtsund et al., 2010].

Droop based topology

The droop control is a well known approach used for power sharing both in strong grids and Microgrids without the need of communication among distributed generation units, which contributes for an easy application. The designed control loop is composed by $P-f$ and $Q-V$ droops considering an electrical grid with inductive impedance ($X >> R$) and large amount of inertia, which is the case of conventional power system with high voltage transmission lines. In the classical case, equations (15.12) and (15.13) model the droop relation. But, when dealing with Microgrids composed of medium and low voltage lines, in many cases the impedance is not inductive ($X \approx R$) and the active and reactive power decoupling is not true. Then, the traditional droop relation ($P-f$ and $Q-V$) is not applicable. In fact, in resistive lines, the reactive power will depend on the phase angle (or frequency) and the voltage is related to the real power exchange. Therefore, an opposite droop may be addressed by $P-V$ and $Q-f$ droops to provide proper power sharing [Chang et al., 2015].

The steady-state equation that relates frequency and active power is given as:

$$\omega_g = \omega^* - m_p(P_m - P^*) \tag{15.12}$$

where ω_g is the grid frequency, P_m is the power in the generator, P^* is the active power set point and ω^* is the grid frequency reference [De Brabandere et al., 2007].

The steady-state equation for voltage droop equation is written as:

$$V = V^* - m_q(Q_m - Q^*) \tag{15.13}$$

where V is the grid voltage amplitude, V^* is the nominal voltage reference, Q_m is the filtered reactive power, Q^* is the reactive power set point [Dohler et al., 2018].

Droop strategy has only steady-state properties, with no dynamical contribution to frequency or voltage regulation. This is because the droop equations only includes frequency and voltage deviation. Therefore, the result is a slow transient response with improper active power sharing. In addition, droop control is not able to bring the system back to the original (or desired) equilibrium point. The inclusion of a frequency derivative term can bring a inertial response for droop strategy, approaching the VSG control scheme and can be compared with the following virtual inertia strategy [De Brabandere et al., 2007, Mohd et al., 2010].

Another approach to provide virtual inertia is to insert a time delay in the active power response, to emulate the inertial behavior of a synchronous machine [Arani et al., 2014]. In droop control applications, the measured output power is filtered to avoid noise and high frequency components from power converter switching. Usually, a low-pass filter with a suitable time constant is applied, so the filter will induce a slower behavior in active and reactive power that can be compared with the inertial behavior of a synchronous machine [Soni et al., 2013]. Consequently, the droop control with a well designed filter may be used for virtual inertia purposes. A standard low-pass filter for active power can be described as follows:

$$P^*_{out}(s) = \frac{1}{1 + sT_f} P_m(s) \tag{15.14}$$

where P^*_{out} is the filtered output active power measured in the system, T_f is the filter time constant and P_m is the measured active power.

[9]PLL performance problems can also be cited here, since may bring steady-state errors and instability mainly in weak grids application. So, this approach requires robust PLL implementation [Svensson, 2001].

According to [D'Arco and Suul, 2013], applying the filter dynamics (15.14) in the frequency droop equation (15.12), we may result in the following expression that presents a virtual inertial component, which is the frequency derivative term:

$$P^*_{out} - P_m = \frac{1}{m_p}(\omega^* - \omega_g) + \frac{T_f}{m_p}\frac{d\omega_g}{dt} \tag{15.15}$$

where the derivative term is equivalent to the inertial response, which results in a low-pass filter with analogous function of a virtual inertia approach. It is necessary to correctly tune the parameters of the droop regulator to obtain a small-signal behavior of a synchronous machine [D'Arco and Suul, 2013].

15.4.2 Virtual Inertia Control Application

The VSM can act to provide transient power sharing and primary frequency support independently, using only local measurements. VSM can also be implemented with no need of PLL, being used just for sensing the grid frequency or during initial machine starting[10]. As result, VSM are conceptually simple thanks to intuitive interpretation as synchronous machines responses [D'Arco et al., 2015a, Tamrakar et al., 2017]. The VSM is implemented to provide frequency reference output, with the power flow been related to inertia emulation and the angle from the swing equation, while voltage amplitude and reactive power control is made separately by the modulation index in the converter. The VSM scheme is introduced in Figure 15.8, where the direct application of VSM concept is built, which means that the voltage amplitude and the phase angle are directly used to generate the PWM signal in the converter [D'Arco and Suul, 2013].

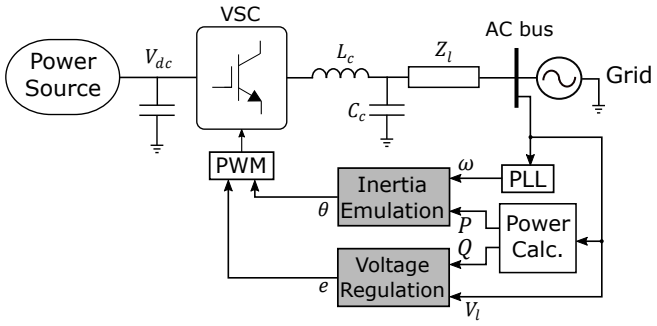

Figure 15.8: VSM general control scheme for a Microgrid integration.

To develop a VSM, it is necessary to implement the swing equation of a Synchronous Machine in the VSC control structure as detailed in [Zhong and Weiss, 2010]. In the following, it is presented the general swing equation of a synchronous machine applied for VSM implementation, where the inertia acceleration is represented by the power balance and a damping factor:

$$\dot{\tilde{\omega}} = \frac{1}{H}[P_{ref} - P - D_p(\omega_{vsm} - \omega_g)] \tag{15.16}$$

where $\tilde{\omega} = \omega_{vsm} - \omega_g$ is the frequency deviation, ω_{vsm} is the VSM's frequency, H the virtual inertia coefficient and D_p the damping factor. P_{ref} is the active power droop reference and P is the measured power into the AC grid.

The inertia coefficient is defined in [Kundur et al., 1994]:

$$H = \frac{J\omega_o^2}{2S_{nom}} \tag{15.17}$$

where S_{nom} is the nominal apparent power of the VSC converter, ω_o is nominal grid value and J is the emulated moment of inertia. In (15.17) it is evident the inverse ratio between moment of inertia and its time constant, H given in seconds.

[10]The swing equation of VSM allows interactions with the grid frequency, influencing its behavior.

The electrical model applied here was developed in two parts: the Microgrid with an output LC filter, and the VSM model. The VSM with proper virtual inertia parameters is applied to improve frequency stability and reduce power oscillations in the grid. The synthetic inertia scheme is incorporated in a VSC converter connected to an AC Microgrid composed by a diesel generator and loads. The DC side of the grid is formed by a DC Microgrid able to provide energy (ancillary services) to the AC side of the grid. The DC side of the grid is summarized here as voltage V_{dc}. The electrical model of the system is depicted in Figure 15.9.

The VSC converter has a LC filter, represented by L_c and C_c, connected to the Point of Common Coupling (PCC) with the AC Microgrid. The line impedance is represented by L_l and the active losses are given by R_l. The state space model of the system can be written as:

$$\dot{I}_{c,d} = -\frac{R_c}{L_c} I_{c,d} + \omega_g I_{c,q} + \frac{1}{2L_c} V_{dc} m_d - \frac{V_{c,d}}{L_c} \tag{15.18}$$

$$\dot{I}_{c,q} = -\frac{R_c}{L_c} I_{c,q} - \omega_g I_{c,d} + \frac{1}{2L_c} V_{dc} m_q - \frac{V_{c,q}}{L_c} \tag{15.19}$$

$$\dot{V}_{c,d} = \frac{I_{c,d}}{C_c} - \frac{I_{l,d}}{C_c} + \omega_g V_{c,q} \tag{15.20}$$

$$\dot{V}_{c,q} = \frac{I_{c,q}}{C_c} - \frac{I_{l,q}}{C_c} - \omega_g V_{c,d} \tag{15.21}$$

$$\dot{I}_{l,d} = -\frac{R_l}{L_l} I_{l,d} + \omega_g I_{l,q} + \frac{V_{c,d}}{L_l} - \frac{V_{l,d}}{L_l} \tag{15.22}$$

$$\dot{I}_{l,q} = -\frac{R_l}{L_l} I_{l,q} - \omega_g I_{l,d} + \frac{V_{c,q}}{L_l} - \frac{V_{l,q}}{L_l} \tag{15.23}$$

$V_{c,dq}$ is the voltage on the LC filter capacitor C_c and $I_{c,dq}$ is the current on inductor L_c. $I_{l,dq}$ is the SRF line current and the modulation indexes are m_d and m_q. V_l is the voltage on the diesel generator and P_{load} and Q_{load} are the active and reactive power demand of the load in the AC Microgrid respectively. The angular speed is given by ω_g, where $\omega_g = 2\pi f_g$.

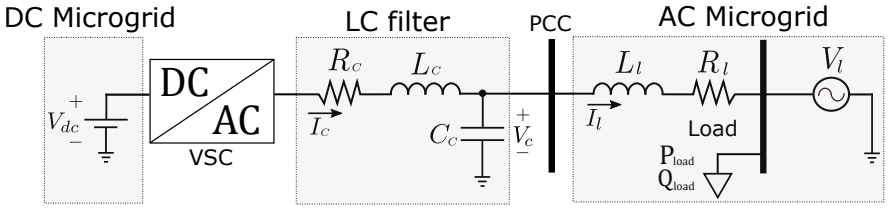

Figure 15.9: Virtual Synchronous Machine (VSM) connected to an AC Microgrid based on diesel generation.

The scheme of the proposed control strategy is composed by the active and reactive power control, given by the droop controllers. The active power control provides the power reference for the swing equation of the virtual inertia to generate the power angle of the converter. Here, the control system is used to directly generate the voltage references for PWM signals driving the power electronic conversion. Modulation indexes (m_d and m_q) provide the signal reference to obtain the desired sinusoidal waveform for voltage and current output (V_c and I_c) on the VSC converter in synchronism the diesel generator, such that, the ancillary services purposes are accomplished.

According to the control target, frequency (ω_{vsm}) and voltage ($V_{c,d}$) are chosen as the control outputs. Modulation indexes (m_d and m_q) provide the reference to generate the PWM signals, where m_d and m_q are transformed into phasor signal with amplitude m and phase θ, chosen as the control inputs. The angle is given by θ_{vsm} from the swing equation in (15.16) and voltage reference $V_{c,d_{ref}}$ is given by the droop strategy in (15.13):

$$\frac{V_{dc}}{2} m \angle\theta = V_{c,d_{ref}} \angle\theta_{vsm} \tag{15.24}$$

The signal obtained in (15.24) is the reference signal for the PWM modulation, making possible to emulate inertia in the VSC.

Stability analysis

The stability analysis of the virtual inertia can be compared with the conventional stability analysis of synchronous machines. The swing equation can be rewritten considering the total inertia of the system and defining $\tilde{\omega} = \omega_{vsm} - \omega_g$:

$$M\dot{\tilde{\omega}} = P_m - P_{max}\sin(\delta) - D\tilde{\omega} \tag{15.25}$$

where δ is the power angle, $P_{max} = |V_{vsm}||V_g|/X_{eq}$ is the maximum power for the remaining of the grid and the VSC converter. D is the equivalent damping factor and M is the equivalent inertia coefficient given by [Gonzalez-Torres et al., 2018]:

$$M = \frac{H_{vsm}H_{grid}}{H_{vsm} + H_{grid}} \tag{15.26}$$

H_{vsm} and H_{grid} are the inertia coefficient of the VSM and the remaining grid respectively.

The equivalent input power is given by:

$$P_m = \frac{H_{grid}P_{vsm} - H_{vsm}P_g}{H_{vsm} + H_{grid}} \tag{15.27}$$

If the damping term is neglected and the swing equation in (15.25) is multiplied by $\tilde{\omega}$, the following equation is arranged [Machowski et al., 2011]:

$$M\tilde{\omega}\dot{\tilde{\omega}} - (P_m - P_{max}\sin\delta)\tilde{\omega} = 0 \tag{15.28}$$

To find a positive function, equation (15.28) is integrated from its equilibrium point ($\delta^e = \bar{\delta}$, $\tilde{\omega}^e = 0$):

$$W_{vi} = \int_0^{\tilde{\omega}} M\tilde{\omega}d\tilde{\omega} - \int_{\bar{\delta}}^{\delta}(P_m - P_{max}\sin\delta)d\delta = C \tag{15.29}$$

where C is a positive constant.

The Lyapunov candidate is given by the energy function of the system [Machowski et al., 2011]:

$$W_{vi} = \tfrac{1}{2}M\tilde{\omega}^2 - [P_m(\delta - \bar{\delta}) + P_{max}(\cos\delta - \cos\bar{\delta})] = \\ E_k + E_p \tag{15.30}$$

where the kinetic energy is given by $E_k = \frac{1}{2}M\tilde{\omega}^2$ and potential energy given by $E_p = -[P_m(\delta - \bar{\delta}) + P_{max}(\cos\delta - \cos\bar{\delta})]$, with respect to the equilibrium points ($\delta^e = \bar{\delta}$, $\tilde{\omega}^e = 0$). The energy function is positive definite around the considered equilibrium point.

The time-derivative of the Lyapunov function can be calculated as follows:

$$\dot{W}_{vi} = \frac{\partial E_k}{\partial\tilde{\omega}}\frac{d\tilde{\omega}}{dt} + \frac{\partial E_p}{\partial\delta}\frac{d\delta}{dt} \tag{15.31}$$

Therefore,

$$\dot{W}_{vi} = \tilde{\omega}M\dot{\tilde{\omega}} - (P_m - P_{max}\sin\delta)\tilde{\omega} - D\tilde{\omega}^2 \tag{15.32}$$

The result is a negative semi-definite function of the time derivative of the Lyapunov function [Bretas and Alberto, 2003].

$$\dot{W}_{vi} = -D\tilde{\omega}^2 < 0 \tag{15.33}$$

where one can see that the energy of the system is dissipated proportionally to the damping factor and the frequency deviation. Therefore, the given equilibrium point can be shown (using Barbalat's Lemma) to be asymptotically stable [Machowski et al., 2011, Kundur et al., 1994].

15.4.3 Application Example

The proposed model was built on *Matlab/Simulink* using *SimScape Electrical* toolbox. The VSC converter interfaces the DC Microgrid to The AC one, which is composed of a diesel generator and loads, as depicted in Figure 15.9. The diesel generator in the AC Microgrid has a Governor (speed control) to control the frequency and active power. The control parameters of the governor are presented as follows: Regulator gain $K = 150$ and time constant $T_{reg} = 0.1s$, actuator time constant $T_{act} = 0.25s$ and engine time delay $T_d = 0.024s$. The AVR is implemented to control the excitation of the machine, terminal voltage and reactive power regulation [Lee, 2016]. The AVR parameters are presented as follows: Voltage regulator gain $K_{va} = 400$, time constant $T_{va} = 0.02s$ and low-pass filter time constant $T_r = 0.02s$.

The VSM and the AC grid parameters are presented in Table 15.2. The nominal frequency of the grid is $f_n = 50Hz$ and the nominal power of the diesel generator is $S_{diesel} = 2MVA$ with $V_l = 400V$ rms nominal voltage, 2 pairs of poles and inertia coefficient of $H_{diesel} = 3s$. The Q-V droop coefficient is $K_q = 0.3$.

Table 15.2: Microgrid parameters

VSC	$S_{nom} = 1MVA$	$f_s = 20kHz$	$\hat{V}_{c,nom} = 400V$
LC Filter	$R_c = 20m\Omega$	$L_c = 0.25mH$	$C_c = 150\mu F$
VSM	$K_w = 20$	$D_p = 50$	$H_o = 2s$
AC grid	$R_l = 0.1\Omega$	$L_l = 0.01mH$	$V_{l,nom} = 400V$

Here, the VSM has a nominal power of $S_{vsm} = 1MVA$ and same nominal rms voltage as the grid $V_{vsm} = 400V$, where these values are the base for per unit transformation. The active and reactive power demand for the load in the Microgrid is introduced in Table 15.3.

Active power (P) and reactive power (Q) injected by the VSC converter are controlled in their references (P^* and Q^*), given by a higher control level, according to power dispatch schedule. The controlled active and reactive power are presented in Figure 15.10. Active power is well controlled, following the reference with small overshoots during the load changes. The reactive power is controlled to maintain the voltage regulated in the desired value, and the reactive power reference is given by a secondary control. The steady-state errors in reactive power are due to the droop control feature.

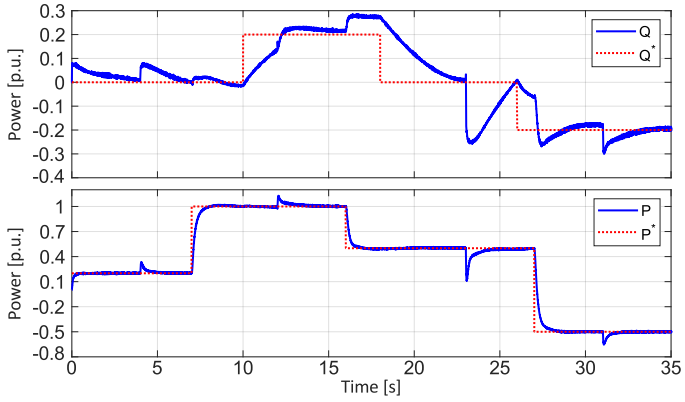

Figure 15.10: The controlled active and reactive power in the VSC converter of the Microgrid.

The VSM have about the same power level of the main generation, given by the synchronous machine. Then, in this case, the operation of the generator is affected by the power converter and the

Table 15.3: The AC load power demand.

Time $[s]$	0	4	12	23	31
Active power $[MW]$	0.5	1	1.8	1.8	1.3
Reactive Power $[kW]$	50	100	200	150	100

dynamic of the system is completely changed, so the power variations in the machine in combination with the VSM assures the stability of the system. The diesel generator has a governor to control the frequency without steady-state error, acting as a primary frequency controller. Voltage and machine excitation are regulated by the AVR control, according with standard paramatrization of the controllers and also ensure the elimination of steady-state error in voltage. Therefore, it is clear that the power response of the synchronous machine is slower than the power variations in the VSM. And, the VSM participates in the operation of the network, contributing to the system stability together with the diesel generator.

The voltage on the PCC is controlled according the $P-V$ voltage droop. The voltage amplitude, given by $V_{c,d}$ is introduced in Figure 15.11, where the overshoots are caused mainly during the load changes and the reactive power reference changes. But, even with deviations, the voltage operates within the established limits

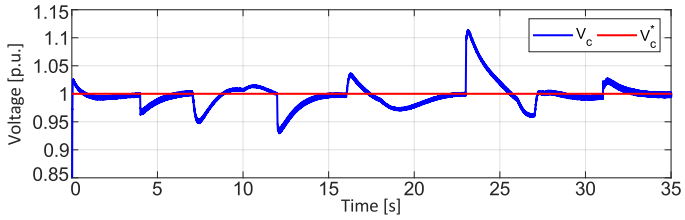

Figure 15.11: The voltage amplitude profile on the PCC.

The frequency of the grid and its reference are depicted in Figure 15.12. The diesel generator has a governor to track the frequency in the desired value, therefore, there is no error in steady-state. The virtual inertia with the droop equation provide the power sharing with the VSM. As result, the frequency has some transient overshoots during load changes and when the active power injection dispatch changes in the VSM, but remains with good transitory behavior, and quick response to disturbances. The VSM provides a better frequency response to the system, decreasing frequency variations improves the speed of convergence during transients.

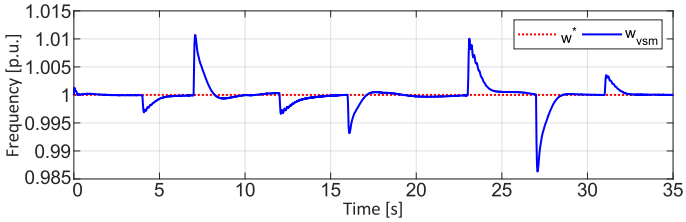

Figure 15.12: The controlled frequency from the VSM approach.

Next, the frequency deviation ($\Delta\omega$) and the frequency RoCoF is introduced in Figure 15.13, where the operational margins of the grid can be analyzed, as the maximum frequency deviation and the rate of change of frequency. These operating margins are given according to the limits imposed by load and power variations, that can trigger load shedding and machine disconnection procedures.

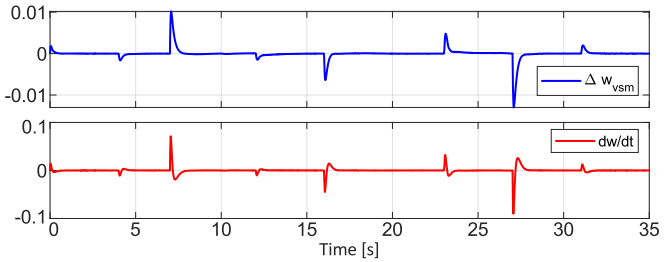

Figure 15.13: The frequency deviation (Δw) and RoCoF.

15.4.4 Isolated operation

In the context of Microgrid operation, errors and failures may exist. In the event of a diesel generator failure, the Microgrid converter must be able to operate stand-alone, controlling the frequency and voltage in the network within the established grid requirements. In this case, it is possible to use the concept of virtual inertia and droop control to maintain the operation of the system. An example is provided here, where only the VSM is supplying the AC loads from the DC side of the Microgrid, i.e., no rotating machines are connected into the system.

Considering the VSM as the main generation, the P and Q dispatch is provided, such that the frequency and the voltage is controlled. Therefore, the reference values of the droop equations (15.12) and (15.13) are set to zero ($P^* = 0$ and $Q^* = 0$). The swing equation of the VSM becomes:

$$\dot{\tilde{\omega}} = \frac{1}{H}[P_{ref} - P - D_p(\omega_{vsm} - \omega^*)] \tag{15.34}$$

where $\tilde{\omega} = \omega_{vsm} - \omega^*$. The swing equation in (15.34) can be applied for isolated operation of the Microgrid. The droop equations can be expressed as follows:

$$P_{ref} = -K_\omega[\omega_{vsm} - \omega^*] \tag{15.35}$$

$$V_{c,d_{ref}} = K_v[V_{c,d} - V^*_{c,d}] - K_q Q \tag{15.36}$$

where K_v is the voltage droop coefficient.

The simulation of the full converter operation is built considering the same Microgrid parameters of previous simulations. Table 15.4 presents the load variation during these simulations. The power generated in the VSM is to attend the load demanded power of the Microgrid, such that the frequency and the voltage are regulated. The active and reactive power injected by the VSM are introduced in Figure 15.14. The power response of the VSM model is slower than the traditional control of power converters, to emulate the behavior of a synchronous machine.

Table 15.4: The AC load power demand in stand-alone operation.

Time $[s]$	0	4	12	23	31
Active power $[MW]$	0.25	0.55	0.9	0.55	0.25
Reactive Power $[kW]$	50	100	200	100	50

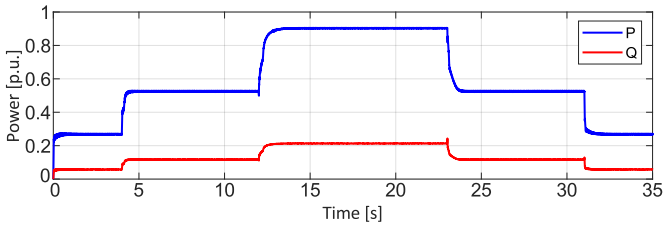

Figure 15.14: The active and reactive power from the VSM in the stand-alone operation.

The voltage on the PCC and the grid frequency are presented in Figure 15.15. The voltage and the frequency present steady-state errors due to droop control behavior. Therefore, when the power demand of the load increases, the voltage and frequency values are stabilized below their references, which can be more clearly seen at 12 and 23 seconds of simulation. The transient overshoots are caused by the load change, with larger variations when compared to the system operating with the diesel generator, where the smallest value of frequency is 48.7 Hz during transients. In this case, the voltage and the frequency varies according to the operating condition of the system, with steady-state errors.

The frequency deviation and the RoCof are depicted in Figure 15.16. In this case, the frequency deviation is much larger than in previous simulations with the diesel generator in operation, and also has a steady-state error. But the frequency RoCoF have smaller peaks when compared with the previous simulations.

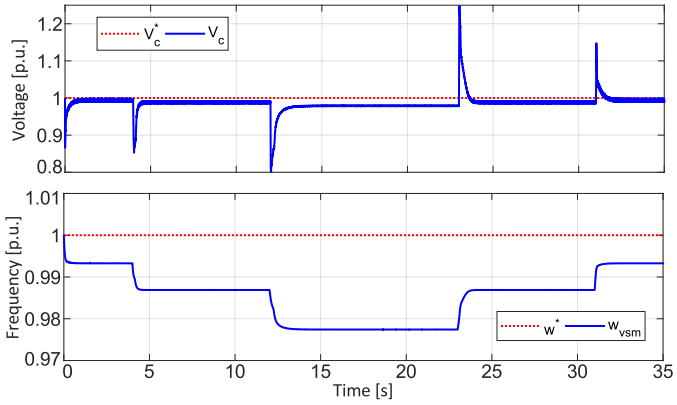

Figure 15.15: The voltage profile and the grid frequency in the stand-alone operation.

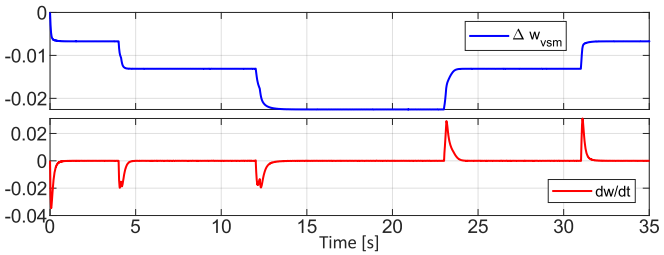

Figure 15.16: Frequency deviation and RoCoF in stand-alone operation.

An integral term from a secondary level control can be inserted in the droop control equations to eliminate the steady-state error of the frequency and the voltage of the system, improving the operating margins and power quality. Therefore, the droop equations are rewritten as follows:

$$P_{ref} = -K_{\omega}[\omega_{vsm} - \omega^*] - K_{\omega}^{\alpha}\alpha_{\omega} \tag{15.37}$$

$$V_{c,d_{ref}} = K_v[V_{c,d} - V_{c,d}^*] - K_q Q - K_v^{\alpha}\alpha_v \tag{15.38}$$

where the integral gains are K_{ω}^{α} and K_v^{α}, the integral terms are given as $\alpha_{\omega} = \int(\omega_{vsm} - \omega^*)dt$ and $\alpha_v = \int(V_{c,d} - V_{c,d}^*)dt$.

The following simulations show the behavior of the system when the integral terms representing the secondary controller are employed. The Microgrid parameters are kept the same and the load variations are presented according to Table 15.4.

The voltage profile on the PCC is introduced in Figure 15.17, where the steady-state error is eliminated by the secondary control, improving the voltage profile. The same behavior can be seen in frequency, where the steady-state error is eliminated, remaining only the transient overshoots during load changes. The transient levels can be reduced according to the secondary control tuning. The frequency behavior with the integral term is introduced in Figure 15.18.

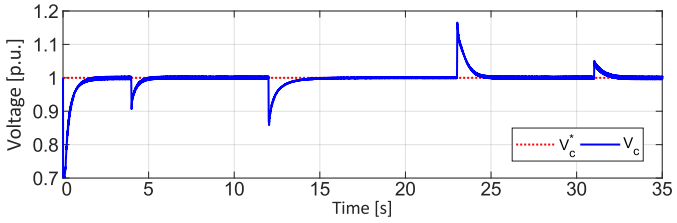

Figure 15.17: Voltage profile on PCC applying the integral term.

The frequency deviation and the RoCoF are presented in Figure 15.19, where frequency deviation is reduced without steady-state error.

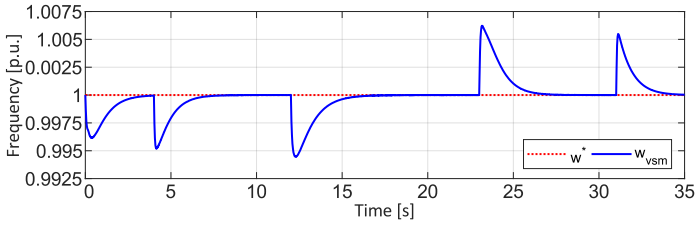

Figure 15.18: Frequency response with the integral term (secondary control).

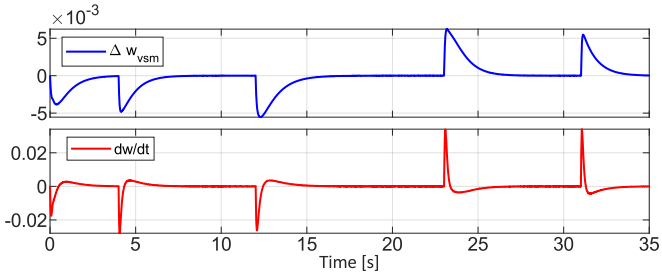

Figure 15.19: Frequency deviation and RoCoF when the integral term is applied.

15.5 Conclusions

In this chapter, an introduction for Microgrid issues is drawn introducing standard control techniques for frequency, inertial stability and power share. The ability of a DC Microgrid to provide ancillary services to an AC grid is highlighted where the virtual inertia approach rise up as a suitable solution for frequency regulation and inertial support. Also, voltage support is given by droop control strategies.

Energy storage and renewable sources technologies may be applied to improve grid support from the DC side of the system. In this way, power converters issues as support to low inertia grids bring great impacts to modern grids affecting the inertial response of the power systems based on power electronic devices. Power converter issues are discussed considering the dynamics of the system and their time-scale properties. The inertial response and the frequency problems are brought to the context of weak grids, where ancillary services can be applied to improve the system operation.

Different virtual inertia approaches are presented in the chapter, where the Virtual Synchronous Machine (VSM) is detailed. A stability analysis for the Synchronous Machine approach is conducted and an application example is provided highlighting the operation combined with traditional synchronous generators and stand-alone operation. The frequency parameters as frequency Nadir and RoCoF are discussed, and inertial support is improved when compared with typical control strategy for power electronic based grids.

Bibliography

[ANEEL, 2018] ANEEL (2018). Resolução normativa 822, de 26 de junho de 2018, que regulamenta a prestação e remuneração de serviços ancilares no sin. Technical report, National Agency of Electrical Energy - ANEEL (Brazil).

[ANEEL, 2019a] ANEEL (2019a). Revisão da resolução normativa 697/2015, que regulamenta a prestação e remuneração de serviços ancilares no sin, relatório de análise de impacto regulatório 006/2019. Technical report, National Agency of Electrical Energy - ANEEL (Brazil).

[ANEEL, 2019b] ANEEL (2019b). Technical arrangements for ancillary services - submodule 14.2. Technical report, National Agency of Electrical Energy - ANEEL (Brazil).

[Arani et al., 2014] Arani, M. F. M., Mohamed, Y. A.-R. I., and El-Saadany, E. F. (2014). Analysis and mitigation of the impacts of asymmetrical virtual inertia. *IEEE Transactions on Power Systems*, 29(6):2862–2874.

[Arnold et al., 2009] Arnold, M., Negenborn, R. R., Andersson, G., and De Schutter, B. (2009). Model-based predictive control applied to multi-carrier energy systems. In *2009 IEEE Power & Energy Society General Meeting*, pages 1–8. IEEE.

[Ashabani and r. I. Mohamed, 2014] Ashabani, S. M. and r. I. Mohamed, Y. A. (2014). New family of microgrid control and management strategies in smart distribution grids; analysis, comparison and testing. *IEEE Transactions on Power Systems*, 29(5):2257–2269.

[Beck and Hesse, 2007] Beck, H. and Hesse, R. (2007). Virtual synchronous machine. In *2007 9th International Conference on Electrical Power Quality and Utilisation*, pages 1–6.

[Bevrani et al., 2017] Bevrani, H., François, B., and Ise, T. (2017). *Microgrid dynamics and control*. John Wiley & Sons.

[Bevrani et al., 2014] Bevrani, H., Ise, T., and Miura, Y. (2014). Virtual synchronous generators: A survey and new perspectives. *International Journal of Electrical Power & Energy Systems*, 54:244–254.

[Bidram and Davoudi, 2012] Bidram, A. and Davoudi, A. (2012). Hierarchical structure of microgrids control system. *IEEE Transactions on Smart Grid*, 3(4):1963–1976.

[Boicea, 2014] Boicea, V. A. (2014). Energy storage technologies: The past and the present. *Proceedings of the IEEE*, 102(11):1777–1794.

[Bordons et al., 2020] Bordons, C., Garcia-Torres, F., and Ridao, M. A. (2020). *Model Predictive Control of Microgrids*. Springer.

[Breithaupt et al., 2016] Breithaupt, T., Tuinema, B., Herwig, D., Wang, D., Hofmann, L., Rueda Torres, J., Mertens, A., Rüberg, S., Meyer, R., Sewdien, V., et al. (2016). Migrate deliverable d1. 1 report on systemic issues. *MIGRATE Project Consortium: Bayreuth, Germany*, page 137.

[Bretas and Alberto, 2003] Bretas, N. G. and Alberto, L. F. (2003). Lyapunov function for power systems with transfer conductances: extension of the invariance principle. *IEEE Transactions on Power Systems*, 18(2):769–777.

[Chang et al., 2015] Chang, C., Gorinevsky, D., and Lall, S. (2015). Stability analysis of distributed power generation with droop inverters. *IEEE Transactions on Power Systems*, 30(6):3295–3303.

[Chen et al., 2014] Chen, Y., Damm, G., Benchaib, A., and Lamnabhi-Lagarrigue, F. (2014). Feedback linearization for the DC voltage control of a VSC-HVDC terminal. In *European Control Conference (ECC)*, pages 1999–2004.

[D'Arco and Suul, 2013] D'Arco, S. and Suul, J. A. (2013). Virtual synchronous machines—classification of implementations and analysis of equivalence to droop controllers for microgrids. In *2013 IEEE Grenoble Conference*, pages 1–7. IEEE.

[De Brabandere et al., 2007] De Brabandere, K., Bolsens, B., Van den Keybus, J., Woyte, A., Driesen, J., and Belmans, R. (2007). A voltage and frequency droop control method for parallel inverters. *IEEE Transactions on power electronics*, 22(4):1107–1115.

[De Brabandere et al., 2007] De Brabandere, K., Bolsens, B., Van den Keybus, J., Woyte, A., Driesen, J., and Belmans, R. (2007). A voltage and frequency droop control method for parallel inverters. *IEEE Transactions on Power Electronics*, 22(4):1107–1115.

[Dohler et al., 2018] Dohler, J. S., de Almeida, P. M., de Oliveira, J. G., et al. (2018). Droop control for power sharing and voltage and frequency regulation in parallel distributed generations on ac microgrid. In *2018 13th IEEE International Conference on Industry Applications (INDUSCON)*, pages 1–6. IEEE.

[Dragičević et al., 2015] Dragičević, T., Lu, X., Vasquez, J. C., and Guerrero, J. M. (2015). Dc microgrids—part i: A review of control strategies and stabilization techniques. *IEEE Transactions on power electronics*, 31(7):4876–4891.

[Dragičević et al., 2016] Dragičević, T., Lu, X., Vasquez, J. C., and Guerrero, J. M. (2016). Dc microgrids—part i: A review of control strategies and stabilization techniques. *IEEE Transactions on power electronics*, 31(7):4876–4891.

[D'Arco et al., 2015a] D'Arco, S., Suul, J. A., and Fosso, O. B. (2015a). Small-signal modeling and parametric sensitivity of a virtual synchronous machine in islanded operation. *International Journal of Electrical Power & Energy Systems*, 72:3–15.

[D'Arco et al., 2015b] D'Arco, S., Suul, J. A., and Fosso, O. B. (2015b). A virtual synchronous machine implementation for distributed control of power converters in smartgrids. *Electric Power Systems Research*, 122:180–197.

[Eirgrid, 2012] Eirgrid, S. (2012). Ds3: System services consultation–new products and contractual arrangements.

[ENTSO-E, 2013] ENTSO-E (2013). Documentation on controller tests in test grid configurations. Technical report, European Network of Transmission System Operators for Electricity.

[ENTSO-E, 2017] ENTSO-E (2017). High penetration of power electronic interfaced power sources (hpopeips). Technical report, Guidance document for national implementation for network codes on grid connection.

[ERCOT, 2013] ERCOT (2013). Future ancillary services in electric reliability council of texas (ercot).

[Gonzalez-Torres et al., 2018] Gonzalez-Torres, J. C., Costan, V., Damm, G., Benchaib, A., Bertinato, A., Poullain, S., Luscan, B., and Lamnabhi-Lagarrigue, F. (2018). Hvdc protection criteria for transient stability of ac systems with embedded hvdc links. *The Journal of Engineering*, 2018(15):956–960.

[Gonzalez-Torres et al., 2020] Gonzalez-Torres, J. C., Damm, G., Costan, V., Benchaib, A., and Lamnabhi-Lagarrigue, F. (2020). Transient stability of power systems withembedded vsc-hvdc links: Stability margins analysis and control. *IET Generation, Transmission & Distribution*.

[Grid, 2014] Grid, N. (2014). Electricity ten year statement. *UK Electricity Transmission, London*.

[Grid, 2016] Grid, N. (2016). Enhanced frequency response: Invitation to tender for pre-qualified parties.

[Iovine et al., 2018] Iovine, A., Jimenez Carrizosa, M., Damm, G., and Alou, P. (2018). Nonlinear Control for DC MicroGrids enabling Efficient Renewable Power Integration and Ancillary Services for AC grids. *IEEE Transactions on Power Systems*, pages 1–1.

[Iovine et al., 2019] Iovine, A., Rigaut, T., Damm, G., De Santis, E., and Di Benedetto, M. D. (2019). Power management for a dc microgrid integrating renewables and storages. *Control Engineering Practice*, 85:59 – 79.

[Iovine et al., 2016] Iovine, A., Siad, S. B., Damm, G., Santis, E. D., and Benedetto, M. D. D. (2016). Nonlinear control of an ac-connected dc microgrid. In *IECON 2016 - 42nd Annual Conference of the IEEE Industrial Electronics Society*, pages 4193–4198.

[Iovine et al., 2017] Iovine, A., Siad, S. B., Damm, G., Santis, E. D., and Benedetto, M. D. D. (2017). Nonlinear control of a dc microgrid for the integration of photovoltaic panels. *IEEE Transactions on Automation Science and Engineering*, 14(2):524–535.

[Jessen et al., 2015] Jessen, L., Günter, S., Fuchs, F. W., Gottschalk, M., and Hinrichs, H.-J. (2015). Measurement results and performance analysis of the grid impedance in different low voltage grids for a wide frequency band to support grid integration of renewables. In *2015 IEEE Energy Conversion Congress and Exposition (ECCE)*, pages 1960–1967. IEEE.

[Jiménez Carrizosa et al., 2018] Jiménez Carrizosa, M., Arzandé, A., Dorado Navas, F., Damm, G., and Vannier, J. C. (2018). A Control Strategy for Multiterminal DC Grids With Renewable Production and Storage Devices. *IEEE Transactions on Sustainable Energy*, 9(2):930–939.

[Joos et al., 2000] Joos, G., Ooi, B., McGillis, D., Galiana, F., and Marceau, R. (2000). The potential of distributed generation to provide ancillary services. In *2000 power engineering society summer meeting (cat. no. 00ch37134)*, volume 3, pages 1762–1767. IEEE.

[Joos et al., 2000] Joos, G., Ooi, B. T., McGillis, D., Galiana, F. D., and Marceau, R. (2000). The potential of distributed generation to provide ancillary services. In *2000 Power Engineering Society Summer Meeting (Cat. No.00CH37134)*, volume 3, pages 1762–1767 vol. 3.

[Kumar et al., 2017] Kumar, D., Zare, F., and Ghosh, A. (2017). Dc microgrid technology: System architectures, ac grid interfaces, grounding schemes, power quality, communication networks, applications, and standardizations aspects. *Ieee Access*, 5:12230–12256.

[Kundur et al., 1994] Kundur, P., Balu, N. J., and Lauby, M. G. (1994). *Power system stability and control*, volume 7. McGraw-hill New York.

[Lee, 2016] Lee, D. (2016). Ieee recommended practice for excitation system models for power system stability studies. *IEEE Std 421.5-2016*, pages 1–207.

[Ma et al., 2012] Ma, Z., Zhong, Q.-C., and Yan, J. D. (2012). Synchronverter-based control strategies for three-phase pwm rectifiers. In *2012 7th IEEE conference on industrial electronics and applications (ICIEA)*, pages 225–230. IEEE.

[Machowski et al., 2011] Machowski, J., Bialek, J., and Bumby, J. (2011). *Power system dynamics: stability and control*. John Wiley & Sons.

[Magne et al., 2012] Magne, P., Nahid-Mobarakeh, B., and Pierfederici, S. (2012). General active global stabilization of multiloads dc-power networks. *IEEE Transactions on Power Electronics*, 27(4):1788–1798.

[Makrygiorgou and Alexandridis, 2017] Makrygiorgou, D. I. and Alexandridis, A. T. (2017). Stability analysis of dc distribution systems with droop-based charge sharing on energy storage devices. *Energies*, 10(4):433.

[Markovic et al., 2019] Markovic, U., Stanojev, O., Vrettos, E., Aristidou, P., and Hug, G. (2019). Understanding stability of low-inertia systems.

[Meng et al., 2017] Meng, L., Shafiee, Q., Trecate, G. F., Karimi, H., Fulwani, D., Lu, X., and Guerrero, J. M. (2017). Review on Control of DC Microgrids and Multiple Microgrid Clusters. *IEEE Journal of Emerging and Selected Topics in Power Electronics*, 5(3):928–948.

[Midtsund et al., 2010] Midtsund, T., Suul, J., and Undeland, T. (2010). Evaluation of current controller performance and stability for voltage source converters connected to a weak grid. In *The 2nd International Symposium on Power Electronics for Distributed Generation Systems*, pages 382–388. IEEE.

[Milano et al., 2018] Milano, F., Dörfler, F., Hug, G., Hill, D. J., and Verbič, G. (2018). Foundations and challenges of low-inertia systems. In *2018 Power Systems Computation Conference (PSCC)*, pages 1–25. IEEE.

[Mohd et al., 2010] Mohd, A., Ortjohann, E., Morton, D., and Omari, O. (2010). Review of control techniques for inverters parallel operation. *Electric Power Systems Research*, 80(12):1477–1487.

[National Grid ESO, 2019] National Grid ESO (2019). Interim report into the low frequency demand disconnection (lfdd) following generator trips and frequency excursion on 9 aug 2019. In *Technical report*.

[Olivares et al., 2014] Olivares, D. E., Mehrizi-Sani, A., Etemadi, A. H., Cañizares, C. A., Iravani, R., Kazerani, M., Hajimiragha, A. H., Gomis-Bellmunt, O., Saeedifard, M., Palma-Behnke, R., Jiménez-Estévez, G. A., and Hatziargyriou, N. D. (2014). Trends in microgrid control. *IEEE Transactions on Smart Grid*, 5(4):1905–1919.

[Parisio et al., 2014] Parisio, A., Rikos, E., and Glielmo, L. (2014). A model predictive control approach to microgrid operation optimization. *IEEE Transactions on Control Systems Technology*, 22(5):1813–1827.

[Pattabiraman et al., 2018] Pattabiraman, D., Lasseter., R. H., and Jahns, T. M. (2018). Comparison of grid following and grid forming control for a high inverter penetration power system. In *2018 IEEE Power Energy Society General Meeting (PESGM)*, pages 1–5.

[Perez et al., 2019a] Perez, F., Damm, G., Ribeiro, P., Lamnabhi-Lagarrigue, F., and Galai-Dol, L. (2019a). A nonlinear distributed control strategy for a dc microgrid using hybrid energy storage for voltage stability. In *2019 IEEE 58th Conference on Decision and Control (CDC)*, pages 5168–5173. IEEE.

[Perez et al., 2019b] Perez, F., Iovine, A., Damm, G., Galai-Dol, L., and Ribeiro, P. (2019b). Regenerative braking control for trains in a dc microgrid using dynamic feedback linearization techniques. *IFAC-PapersOnLine*, 52(4):401–406.

[Perez et al., 2018] Perez, F., Iovine, A., Damm, G., and Ribeiro, P. (2018). DC microgrid voltage stability by dynamic feedback linearization. In *2018 IEEE International Conference on Industrial Technology (ICIT)*, pages 129–134.

[Poolla et al., 2019] Poolla, B. K., Groß, D., and Dörfler, F. (2019). Placement and implementation of grid-forming and grid-following virtual inertia and fast frequency response. *IEEE Transactions on Power Systems*, 34(4):3035–3046.

[Rebours et al., 2007] Rebours, Y. G., Kirschen, D. S., Trotignon, M., and Rossignol, S. (2007). A survey of frequency and voltage control ancillary services—part ii: Economic features. *IEEE Transactions on power systems*, 22(1):358–366.

[Rodrigues Lima, 2017] Rodrigues Lima, J. (2017). *Variable speed pumped storage plants multi-time scale control to allow its use to power system stability*. PhD thesis, Paris Saclay.

[Sahoo et al., 2017] Sahoo, S. K., Sinha, A. K., and Kishore, N. (2017). Control techniques in ac, dc, and hybrid ac-dc microgrid: a review. *IEEE Journal of Emerging and Selected Topics in Power Electronics*, 6(2):738–759.

[Sakimoto et al., 2011] Sakimoto, K., Miura, Y., and Ise, T. (2011). Stabilization of a power system with a distributed generator by a virtual synchronous generator function. In *8th International Conference on Power Electronics-ECCE Asia*, pages 1498–1505. IEEE.

[Shrestha et al., 2017] Shrestha, D., Tamrakar, U., Ni, Z., and Tonkoski, R. (2017). Experimental verification of virtual inertia in diesel generator based microgrids. In *2017 IEEE International Conference on Industrial Technology (ICIT)*, pages 95–100. IEEE.

[Soni et al., 2013] Soni, N., Doolla, S., and Chandorkar, M. C. (2013). Improvement of transient response in microgrids using virtual inertia. *IEEE transactions on power delivery*, 28(3):1830–1838.

[Svensson, 2001] Svensson, J. (2001). Synchronisation methods for grid-connected voltage source converters. *IEE Proceedings-Generation, Transmission and Distribution*, 148(3):229–235.

[Tahim et al., 2015] Tahim, A. P. N., Pagano, D. J., Lenz, E., and Stramosk, V. (2015). Modeling and stability analysis of islanded dc microgrids under droop control. *IEEE Transactions on Power Electronics*, 30(8):4597–4607.

[Tamrakar et al., 2017] Tamrakar, U., Shrestha, D., Maharjan, M., Bhattarai, B. P., Hansen, T. M., and Tonkoski, R. (2017). Virtual inertia: Current trends and future directions. *Applied Sciences*, 7(7):654.

[Tayab et al., 2017] Tayab, U. B., Roslan, M. A. B., Hwai, L. J., and Kashif, M. (2017). A review of droop control techniques for microgrid. *Renewable and Sustainable Energy Reviews*, 76:717–727.

[Tielens and Van Hertem, 2016] Tielens, P. and Van Hertem, D. (2016). The relevance of inertia in power systems. *Renewable and Sustainable Energy Reviews*, 55:999–1009.

[Torres and Lopes, 2009] Torres, M. and Lopes, L. A. (2009). Virtual synchronous generator control in autonomous wind-diesel power systems. In *2009 IEEE Electrical Power & Energy Conference (EPEC)*, pages 1–6. IEEE.

[Torres and Lopes, 2013] Torres, M. and Lopes, L. A. (2013). Virtual synchronous generator: A control strategy to improve dynamic frequency control in autonomous power systems.

[Tucci et al., 2016] Tucci, M., Riverso, S., Vasquez, J. C., Guerrero, J. M., and Ferrari-Trecate, G. (2016). A decentralized scalable approach to voltage control of dc islanded microgrids. *IEEE Transactions on Control Systems Technology*, 24(6):1965–1979.

[Van et al., 2010] Van, T. V., Visscher, K., Diaz, J., Karapanos, V., Woyte, A., Albu, M., Bozelie, J., Loix, T., and Federenciuc, D. (2010). Virtual synchronous generator: An element of future grids. In *2010 IEEE PES Innovative Smart Grid Technologies Conference Europe (ISGT Europe)*, pages 1–7. IEEE.

[Van Wesenbeeck et al., 2009] Van Wesenbeeck, M., De Haan, S., Varela, P., and Visscher, K. (2009). Grid tied converter with virtual kinetic storage. In *2009 IEEE Bucharest PowerTech*, pages 1–7. IEEE.

[Vasquez et al., 2010] Vasquez, J. C., Guerrero, J. M., Miret, J., Castilla, M., and De Vicuna, L. G. (2010). Hierarchical control of intelligent microgrids. *IEEE Industrial Electronics Magazine*, 4(4):23–29.

[Winter et al., 2014] Winter, W., Elkington, K., Bareux, G., and Kostevc, J. (2014). Pushing the limits: Europe's new grid: Innovative tools to combat transmission bottlenecks and reduced inertia. *IEEE Power and Energy Magazine*, 13(1):60–74.

[Wu et al., 2004] Wu, T., Rothleder, M., Alaywan, Z., and Papalexopoulos, A. D. (2004). Pricing energy and ancillary services in integrated market systems by an optimal power flow. *IEEE Transactions on power systems*, 19(1):339–347.

[Yang et al., 2016] Yang, N., Nahid-Mobarakeh, B., Gao, F., Paire, D., Miraoui, A., and Liu, W. (2016). Modeling and stability analysis of multi-time scale dc microgrid. *Electric Power Systems Research*, 140:906–916.

[Zhong, 2016] Zhong, Q.-C. (2016). Virtual synchronous machines: A unified interface for grid integration. *IEEE Power Electronics Magazine*, 3(4):18–27.

[Zhong et al., 2013] Zhong, Q.-C., Nguyen, P.-L., Ma, Z., and Sheng, W. (2013). Self-synchronized synchronverters: Inverters without a dedicated synchronization unit. *IEEE Transactions on power electronics*, 29(2):617–630.

[Zhong and Weiss, 2010] Zhong, Q.-C. and Weiss, G. (2010). Synchronverters: Inverters that mimic synchronous generators. *IEEE Transactions on Industrial Electronics*, 58(4):1259–1267.